Modeling the thermopower of icosahedral $Al_{63}Cu_{25}Fe_{12}$ quasicrystals: Spectral fine structure

Enrique Maciá*
Departamento de Física de Materiales, Facultad de Físicas, Universidad Complutense, E-28040 Madrid, Spain
(Received 16 July 2003; revised manuscript received 21 November 2003; published 15 April 2004)

On the basis of a realistic model for the spectral conductivity, obtained from a proper combination of tunneling spectroscopy [R. Escudero *et al.*, J. Phys.: Condens. Matter **11**, 383 (1999)] and transport measurements, we derive a closed analytical expression for the Seebeck coefficient, satisfactorily describing its temperature dependence over a wide temperature range. The relative importance of thermal broadening effects and the temperature dependence of chemical potential in the thermopower curve is quantitatively discussed. By comparing the obtained analytical results with the experimental $S(T)$ curve evidence for band structure effects in the thermopower is reported.

DOI: 10.1103/PhysRevB.69.132201 PACS number(s): 61.44.Br, 71.20.−b, 72.10.−d

Attending to their transport properties thermodynamically stable icosahedral quasicrystals (QC's) occupy an odd position among the well-ordered condensed-matter phases. In fact, by comparing the temperature and composition dependences of electrical conductivity, thermal conductivity, thermoelectric power, and Hall coefficient of quasicrystalline alloys with those corresponding to both crystalline and amorphous alloys of similar composition, several anomalous behaviors have been reported.[1–5] These anomalies clearly resemble a more semiconductorlike than metallic character,[6–8] although typical metallic fingerprints, like the presence of a well-defined Fermi edge[9] or an ideal Ohmic behavior over a broad voltage range,[10] have been observed in high-quality icosahedral samples. Therefore, neither the notion of metal nor that of a conventional semiconductor seem to be suitable for QC's.

Following a systematic theoretical study, aimed to ascertain the influence of the electronic structure on the transport coefficients of icosahedral QC's, we have introduced a phenomenological approach relating the sample's electronic structure to the temperature dependence of several transport coefficients.[11–14] The main aim of this work is to relate some key topological features in the experimental thermopower curve to a few characteristic features in the electronic structure. To this end, we shall consider thermal broadening effects and the variation of the chemical potential with the temperature in order to derive closed analytical expressions for the thermopower in terms of a set of phenomenological coefficients and compare them with suitable experimental data.

The temperature dependence of the thermoelectric power $S(T)$ can be obtained by means of the Chester-Thellung-Kubo-Greenwood version of the linear-response theory from the expression[15]

$$S(T)=\frac{1}{|e|T}\frac{\mathcal{L}_{12}(T)}{\mathcal{L}_{11}(T)}, \tag{1}$$

where e is the electron charge, T is the temperature, and the kinetic coefficients are given by

$$\mathcal{L}_{ij}(T)=(-1)^{i+j}\int_{-\infty}^{+\infty}dE\,\sigma(E)(E-\mu)^{i+j-2}\left(-\frac{\partial f}{\partial E}\right), \tag{2}$$

where $f(E,\mu,T)$ is the Fermi-Dirac distribution function and $\mu(T)$ is the chemical potential. Our study will focus on the relationship between the conductivity spectrum $\sigma(E)$ and the transport properties. Häussler and collaborators showed that the main qualitative features of the $\sigma(T)$, $S(T)$, and $R_H(T)$ curves for both QC's and their crystalline approximants, can be accounted for by considering an asymmetric $\sigma(E)$ curve characterized by a broad minimum exhibiting a pronounced dip within it.[16] Landauro and Solbrig have shown that a spectral conductivity model including just a wide and a narrow Lorentzian peaks suffices to properly fit the experimental $\sigma(T)$ and $S(T)$ curves of i-$Al_{62.5}Cu_{25}Fe_{12.5}$ over a broad temperature range.[17] Accordingly, we shall consider the following expression for the spectral conductivity:[14,17,18]

$$\sigma(E)=\frac{B}{\pi}\left\{\frac{\gamma_1}{(E-\mu-\delta_1)^2+\gamma_1^2}+\alpha\frac{\gamma_2}{(E-\mu-\delta_2)^2+\gamma_2^2}\right\}^{-1}. \tag{3}$$

This model consists of just two main spectral features and it involves six parameters, $\{B,\alpha,\gamma_1,\gamma_2,\delta_1,\delta_2\}$, determining the Lorentzians' half-widths (γ_i) and heights $h_i=(\pi\gamma_i)^{-1}$, their positions (δ_i) with respect to the Fermi level, and their relative weight in the overall electronic structure (α). The parameter B is a scale factor expressed in $\Omega^{-1}\mathrm{cm}^{-1}\mathrm{eV}^{-1}$ units.

Making use of Eq. (3), assuming $\mu\simeq E_F$ and keeping terms up to $O(T^4)$, we have previously obtained[12,13]

$$S(T)=-2|e|\mathcal{L}_0T\frac{\xi_1+\xi_3bT^2}{1+\xi_2bT^2+\xi_4b^2T^4}, \tag{4}$$

where $\mathcal{L}_0=\pi^2k_B^2/3e^2$ is the Lorenz number, $b\equiv e^2\mathcal{L}_0=2.44\times10^{-8}$ $(\mathrm{eV})^2\,\mathrm{K}^{-2}$, and the phenomenological coefficients were defined in Ref. 12. The coefficient ξ_1 is related to topology of the spectral conductivity around the Fermi level through the expression[11,13]

$$\xi_1=\frac{1}{2}\left(\frac{d\ln\sigma(E)}{dE}\right)_{E=\mu}, \tag{5}$$

so that its precise value is very sensitive to the relative position of the Fermi level with respect to the dip minimum.

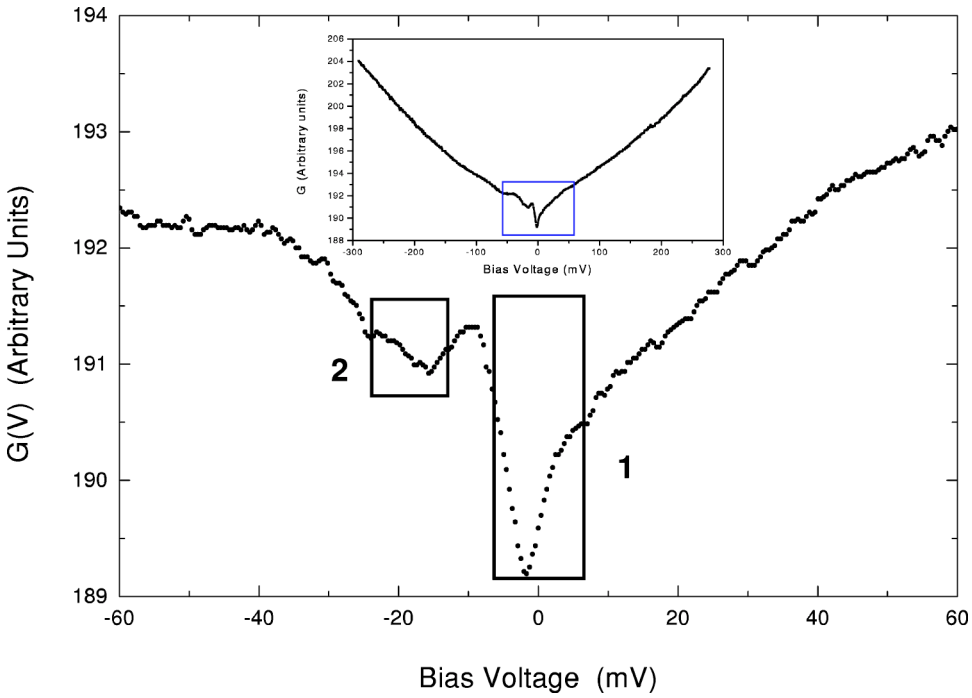

FIG. 1. The differential conductance for the $Al_{63}Cu_{25}Fe_{12}$-Al tunnel junction at a temperature of $T=2$ K at two different energy scales: ± 60 meV (main frame) and ± 300 meV (inset). The boxes labeled 1 and 2 highlight the main spectral features considered in our study. See the main text for more details. Data file, courtesy of R. Escudero.

Similarly, the temperature dependence of the chemical potential is also sensitive to possible fine structures in the density of states (DOS) through the expression[19] $\mu(T) \simeq E_F - \eta T^2$, where

$$\eta = \frac{b}{2}\left(\frac{1}{N(E)}\frac{dN(E)}{dE}\right)_{E_F} \simeq b\xi_1, \tag{6}$$

and $N(E)$ is the DOS. In obtaining Eq. (6) we have assumed an almost constant spectral diffusivity, $D(E) \simeq D_0$, close to the Fermi level, so that $N(E) \simeq \sigma(E)/e^2 D_0$ in a first approximation.[20] This simplifying assumption is experimentally supported by diffusivity estimations from specific-heat data,[21] and by angle-resolved photoelectron spectra showing flat narrow bandlike features indicating quite small group velocities for the charge carriers.[22] Then, Eq. (1) can be expressed as

$$\tilde{S}(T) = -\frac{k_B}{|e|}\left(\frac{\tilde{J}_1}{\tilde{J}_0} + 2\omega\right), \tag{7}$$

where $2\omega \equiv \pi^2 \beta^{-1} \xi_1/3$, and the reduced kinetic coefficients are given by

$$\tilde{J}_n(\beta) = \int x^n \sigma(x) \mathrm{sech}^2(x/2+\omega) dx, \tag{8}$$

where $x \equiv \beta(E-E_F)$ and $\beta \equiv (k_B T)^{-1}$. Following the procedure introduced in Refs. 12 and 14, keeping terms up to $O(T^6)$, we finally obtain,

$$S(T) = -2|e|\mathcal{L}_0 \xi_1 T \tilde{D}(T), \tag{9}$$

where

$$\tilde{D}(T) \equiv \frac{1 - \xi_2 b T^2 - \frac{5}{7}\xi_1 \xi_3 b^2 T^4 - \frac{5}{21}\xi_1^3 \xi_3 b^3 T^6}{1 + (\xi_2 - 2\xi_1^2) b T^2 + (\xi_1 \xi_2 - \frac{10}{7}\xi_3)\xi_1 b^2 T^4 - \frac{10}{21}\xi_1^3 \xi_3 b^3 T^6}. \tag{10}$$

According to Eqs. (10) and (5) in the low-temperature limit $[\tilde{D}(T \to 0) = 1]$ we recover the usual Mott's expression. Then making use of the experimentally measured slope of the $S(T)$ curve in the low-temperature regime, m_0, the phenomenological coefficient ξ_1 can be obtained as[12] $\xi_1^{\mathrm{expt}} \simeq -20.5 m_0$ $[\mu \mathrm{V\,K}^{-2}]$, $(\mathrm{eV})^{-1}$. By comparing Eqs. (4) and (9) we see that the chemical-potential temperature dependence, rather than describing a minor correction, has a significant influence on the thermoelectric power curve. In particular, at high enough temperatures $[\tilde{D}(T \to \infty) = 1/2]$ Eq. (10) prescribes a linear temperature dependence of the thermopower given by $S(T) = |e|\mathcal{L}_0 \xi_1 T \equiv m_\infty T$. Between both linear regimes, which are characterized by different slopes $(m_0/m_\infty = 2)$, the thermoelectric power exhibits a nonlinear behavior, characterized by the presence of well-defined extrema and sign changes.

As an illustrative example we will consider the quasicrystalline sample i-$Al_{63}Cu_{25}Fe_{12}$. Tunneling spectroscopy mea-

surements for this sample[23] are shown in Fig. 1. These measurements reveal a broad pseudogap extending over an energy scale of about 0.6 eV (shown in the inset) along with some fine structure close to the Fermi level (labeled 1 and 2 in the main frame). Consequently, we have *two dips* embedded within a broader pseudogap. This pseudogap stems from a Fermi surface pseudo-Jones zone interaction, while the dips may be related to hybridization effects between *d*-Fe states and *sp*-states. In this sense, a reasonable explanation for the observation of fine structure at certain locations of the sample is that in those tunneling areas there may be portions of material with a better structural quasicrystalline quality than other parts of the same sample,[23] hence favoring energy resonant effects in the iron subsystem.[18,24]

However, data obtained from low-temperature tunnel fits are to be used carefully when extrapolated to describe the temperature dependence of transport coefficients. In fact, the stability of finer spectral features obtained from *ab initio* calculations was discussed by Landauro and Solbrig showing that half-width values obtained for narrowest spectral features become meaningless as they progressively broaden as the temperature increases.[17,24,25] Indeed, a thermal broadening of the dip around the Fermi level has been experimentally reported by Escudero and co-workers for different quasicrystalline samples.[23] In order to properly account for these effects, the width of the narrowest spectral feature will be determined from the expression defining ξ_1 (Ref. 12) by taking into account physical information contained in the thermopower curve, which is extremely sensitive to the finer details in the electronic structure, through the expression

$$A\gamma_2^4 + C\gamma_2^2 + D = 0, \tag{11}$$

where $A \equiv \gamma_1^2\delta_1 + \xi_1^{\text{expt}}\varepsilon_1^2(\gamma_1^2 + \lambda\varepsilon_1^2)$, $C \equiv \delta_2[2\gamma_1^2\delta_1\delta_2 + \lambda\varepsilon_1^4 + \xi_1^{\text{expt}}\varepsilon_1^2\delta_2(2\gamma_1^2 + \lambda\varepsilon_1^2)]$, $D \equiv \gamma_1^2\delta_2^4(\delta_1 + \xi_1^{\text{expt}}\varepsilon_1^2)$, and $\lambda \equiv h_2/h_1$. From a fitting analysis of the data shown in Fig. 1 we have $\gamma_1 = 587 \pm 1$ meV, $\delta_1 = -5.2 \pm 0.5$ meV, $\delta_2 = -16.1 \pm 0.5$ meV, and $\lambda = 11.41 \pm 0.02$. From a linear fit to the thermopower data shown in Fig. 2, in the temperature range 6–70 K, we obtain $m_0 = -0.219 \pm 0.002\ \mu\text{V K}^{-2} \Rightarrow \xi_1^{\text{expt}} = +4.49 \pm 0.03\ (\text{eV})^{-1}$, so that we get $\eta = 1.1 \times 10^{-7}\ \text{eV K}^{-2}$, in close agreement with the value $\eta = 1.0 \times 10^{-7}\ \text{eV K}^{-2}$ previously reported.[17] Plugging the obtained γ_1, δ_1, δ_2, and ξ_1^{expt} values into Eq. (11) we finally get $\gamma_2 = 55 \pm 1$ meV. This value is about eight times larger than the value directly obtained from tunneling measurements, namely, $\gamma_2^0 = 7$ meV at 2 K, hence confirming the importance of thermal broadening effects. From the knowledge of γ_2, the relative weight of both Lorentzian peaks is then determined from the expression (also derived from the expression defining ξ_1)

$$\alpha = -\frac{\gamma_1}{\gamma_2}\left(\frac{\varepsilon_2}{\varepsilon_1}\right)^4 \frac{\delta_1 + \xi_1^{\text{expt}}\varepsilon_1^2}{\delta_2 + \xi_1^{\text{exp}}\varepsilon_2^2}, \tag{12}$$

giving $\alpha = 1.07 \pm 0.03$, in agreement with the value obtained for i-$Al_{62.5}Cu_{25}Fe_{12.5}$ by Landauro and Solbrig.[17] Finally, the conductivity scale parameter B can be determined from the knowledge of the residual conductivity value $\sigma(0)$ as[11]

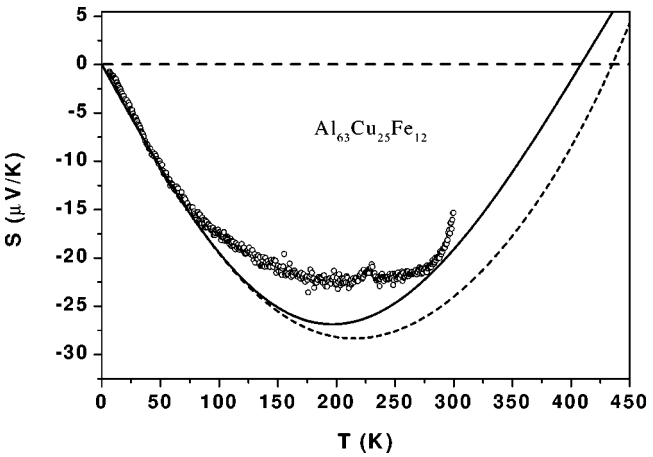

FIG. 2. Comparison between the temperature dependence of the Seebeck coefficient of $Al_{63}Cu_{25}Fe_{12}$ quasicrystal in the temperature range 1–300 K as determined from experiment (open circles) and the analytical expressions given by Eq. (4) (dashed line) and Eq. (9) (solid line). Experimental data, courtesy of R. Escudero.

$$B = \frac{\sigma(0)}{\pi}(\gamma_1\varepsilon_1^{-2} + \alpha\gamma_2\varepsilon_2^{-2}) \quad (\Omega^{-1}\ \text{cm}^{-1}\ \text{eV}^{-1}). \tag{13}$$

Taking the low-temperature electrical conductivity value $\sigma(4.2\ \text{K}) = 188\Omega^{-1}\ \text{cm}^{-1}$ measured for an i-$Al_{63}Cu_{25}Fe_{12}$ sample,[26] we get $B = 1180 \pm 90\Omega^{-1}\ \text{cm}^{-1}\ \text{eV}^{-1}$.

In Fig. 2 we compare the thermopower curve measured by Morales and Escudero[27] (open circles) with the analytical expressions given by Eqs. (4) (dashed line) and (9) (solid line). At low temperatures $S(T)$ follows a linear behavior up to about $T_1 \simeq 70$ K. At higher temperatures the thermopower progressively deviates from linearity, showing a broad minimum. Finally, as the temperature is further increased the $S(T)$ curve steadily increases, suggesting the probable existence of a crossing point where the thermoelectric power will change its sign. The experimental data do not allow for an accurate estimate of this crossing temperature. By extrapolating the $S(T)$ data reported by Bilušic and co-workers[21] for a sample with the same stoichiometry over a wider temperature range we get $T_0^{\text{expt}} \simeq 398$ K. The crossing temperature obtained from Eq. (10) is $T_0 = 408$ K, in good agreement with the extrapolated figure.

By comparing Figs. 1 and 2, we can gain some physical insight into the relationship between the electronic structure and transport properties. First, we note that the deviation from the linear behavior starts when the thermal window reaches a half-width of about $\Delta E \simeq k_B T_1 = 6.0$ meV. This value is close to the spectral peak position $\delta_1 = -5.2$ meV, hence suggesting that as far as the thermal window remains located *inside* the pseudogap's dip feature, the thermopower exhibits a metalliclike behavior. Then, as temperature increases and charge carriers located at the little bump between both dip features start to play a more significant role in the transport properties, the $S(T)$ curve progressively deviates from linear behavior, attaining a broad minimum. This minimum expands from about $T \simeq 175$ ($\Delta E \simeq 15$ meV) up to $T \simeq 275$ ($\Delta E \simeq 24$ meV). The $S(T)$ minimum position can be

related to the different phenomenological coefficients by imposing the extreme condition $dS(T)/dT=0$. From Eq. (9) we obtain $T_2=196$ K, in reasonable agreement with the experimental value $T_2^{\text{expt}}=216$ K (determined from a 4th degree polynomial fitting). The thermal window half-width for this temperature is $\Delta E \simeq k_B T_2 = 16.9$ meV. This value is very close to the spectral resistivity peak position $\delta_2 = -16.1$ meV, hence suggesting that the minimum of the thermopower occurs when the charge carriers located *within* the second dip spectral feature (box 2 in Fig. 2) are playing a major role in the transport properties. Afterwards, as the temperature is further increased and the states belonging to the broad pseudogap component begin to contribute significantly to transport the thermoelectric curve progressively rises towards positive values.

By inspecting Fig. 2 we see that the overall behavior of the theoretically derived $S(T)$ curve given by Eq. (9) provides an acceptable description of the thermoelectric power temperature curve for the icosahedral $Al_{63}Cu_{25}Fe_{12}$ sample, although we cannot obtain a precise match with the experimental one. Then we conclude that, for temperatures higher than $T \simeq 125$ K, the temperature dependence of chemical potential, $\mu(T)$ must be explicitly included in the calculations in order to properly describe the thermoelectric curve. The second main result of this work regards the physical scenario provided by the correlation between some topological features in the $S(T)$ curve—linear regime, broad minimum—and the existence of two fine spectral features in the electronic structure of the sample. In fact, we report on a progressive transition from metalliclike to semiconductorlike thermopower signatures as the Fermi level shifts through both spectral features due to a progressive temperature increase. In this way, we further substantiate some ideas earlier discussed by Pierce *et al.*[28] and Fujiwara *et al.*,[29] who *qualitatively* explained some experimental trends of thermopower in terms of band structure effects. Finally, in this work we illustrate the potential of our phenomenological framework in order to gain information about the electronic structure of quasicrystalline samples from the study of the experimental $S(T)$ curves over a broad temperature range. Within our approach further refinement of the electronic structure model can be obtained from the experimental knowledge of additional phenomenological coefficients. To this end, one reasonably expects then that a sharper view about the main electronic features of the considered QC samples would ultimately emerge from a combined study of the different transport coefficients, $\sigma(T)$, $S(T)$, and $R_H(T)$, over different temperature ranges. The physical information gained in this way may help to clarify the possible existence of finer details in the electronic structure of quasicrystalline samples, like the much debated spiky features, which remain a fundamental open question in the science of QC's.

I warmly thank Professor R. Escudero for sharing his experimental data files and for fruitful discussions. I also thank Professor H. Solbrig for enlightening discussions. I am indebted to Dr. C. V. Landauro for interesting conversations and for sharing useful materials. I acknowledge M. V. Hernández for a critical reading of the manuscript. This work is supported by UCM through Project No. PR3/04-12450.

*Electronic address: emaciaba@fis.ucm.es

[1] S. Roche *et al.*, in *Quasicrystals: An Introduction to Structure, Physical Properties and Applications*, edited by J.B. Suck *et al.*, Springer Series in Materials Science Vol. 55 (Springer-Verlag, Berlin, 2002), p. 321; R. Haberken, *ibid.*, p. 364.
[2] E. Maciá *et al.*, *Ullmann's Encyclopedia of Industrial Chemistry*, 6th ed. (Wiley-VCH, Weinheim, 2002).
[3] Ö. Rapp, in *Physical Properties of Quasicrystals*, edited by Z.M. Stadnik, Springer Series in Solid-State Physics Vol. 126 (Springer-Verlag, Berlin, 1999), p. 127.
[4] J.M. Dubois *et al.*, J. Mater. Res. **8**, 38 (1993).
[5] M.A. Chernikov *et al.*, Phys. Rev. B **51**, 153 (1995); P.A. Kalugin *et al.*, *ibid.* **53**, 14 145 (1996).
[6] K. Kirihara and K. Kimura, Sci. Tech. Adv. Materials **1**, 227 (2000); R. Tamura *et al.*, Phys. Rev. B **50**, 9640 (1994).
[7] T. Klein *et al.*, Phys. Rev. Lett. **66**, 2907 (1991).
[8] A. Carlsson, Nature (London) **353**, 353 (1991).
[9] Z.M. Stadnik *et al.*, Phys. Rev. B **64**, 214202 (2001); Z.M. Stadnik, in *Physical Properties of Quasicrystals* (Ref. 3), p. 257.
[10] T. Klein and O.G. Symko, Phys. Rev. Lett. **73**, 2248 (1994).
[11] E. Maciá, Phys. Rev. B **66**, 174203 (2002).
[12] E. Maciá, J. Appl. Phys. **93**, 1014 (2003).
[13] E. Maciá, Appl. Phys. Lett. **81**, 88 (2002).
[14] C.V. Landauro *et al.*, Phys. Rev. B **67**, 184206 (2003).
[15] R. Kubo, J. Phys. Soc. Jpn. **12**, 570 (1957); D.A. Greenwood, Proc. Phys. Soc. Jpn. **71**, 585 (1958); G.V. Chester and A. Thellung, *ibid.* **77**, 1005 (1961).
[16] P. Häussler *et al.*, J. Alloys Compd. **342**, 228 (2002); P. Häussler *et al.*, Mater. Sci. Eng. **294-296**, 283 (2000); C. Roth *et al.*, J. Non-Cryst. Solids **252**, 869 (1999).
[17] C.V. Landauro and H. Solbrig, Physica B **301**, 267 (2001).
[18] H. Solbrig and C.V. Landauro, Physica B **292**, 47 (2000); C.V. Landauro and H. Solbrig, Mater. Sci. Eng., A **294-296**, 600 (2000).
[19] N. Ashcroft and N. Mermin, *Solid State Physics* (Saunders College Publishing, Orlando, FL, 1976).
[20] E. Maciá, Phys. Rev. B **61**, 8771 (2000).
[21] A. Bilušic *et al.*, Vacuum **61**, 345 (2001); A. Bilušic *et al.*, Mater. Sci. Eng., A **294-296**, 711 (2000).
[22] X. Wu *et al.*, Phys. Rev. Lett. **75**, 4540 (1995).
[23] R. Escudero *et al.*, J. Phys.: Condens. Matter **11**, 383 (1999).
[24] H. Solbrig and C.V. Landauro, *Advances in Solid State Physics*, edited by B. Kramer, Vol. 42 (Springer-Verlag, Berlin, 2002), p. 151.
[25] C.V. Landauro, Ph.D. thesis, Technische Universität Chemnitz, 2002.
[26] A. Sahnoune, J.O. Ström-Olsen, and A. Zaluska, Phys. Rev. B **46**, 10 629 (1992).
[27] F. Morales and R. Escudero, Bull. Am. Phys. Soc. **44**, 1 (1999).
[28] F.S. Pierce *et al.*, Phys. Rev. B **47**, 5670 (1993).
[29] T. Fujiwara *et al.*, Phys. Rev. Lett. **71**, 4166 (1993); T. Fujiwara, J. Non-Cryst. Solids **156-158**, 865 (1993).